

# Recording and Analyzing Multimodal Large-Scale Neuronal Ensemble Dynamics on CMOS-Integrated High-Density Microelectrode Array

Brett Addison Emery<sup>\*1</sup>, Shahrukh Khanzada<sup>\*1</sup>, Xin Hu<sup>\*1</sup>, Diana Klütsch<sup>1</sup>, Hayder Amin<sup>1,2,3</sup>

<sup>1</sup> Group of "Biohybrid Neuroelectronics (BIONICS)", German Center for Neurodegenerative Diseases (DZNE) <sup>2</sup> Faculty of Medicine Carl Gustav Carus, Technical University Dresden <sup>3</sup> Dresden Center for Intelligent Materials (DCIM), Technical University Dresden

\*These authors contributed equally

## Corresponding Author

Hayder Amin

hayder.amin@dzne.de

## Citation

Emery, B.A., Khanzada, S., Hu, X., Klütsch, D., Amin, H. Recording and Analyzing Multimodal Large-Scale Neuronal Ensemble Dynamics on CMOS-Integrated High-Density Microelectrode Array. *J. Vis. Exp.* (2025), e66473, doi:10.3791/66473 (2024).

## Date Published

March 8, 2024

## DOI

10.3791/66473

## URL

jove.com/video/66473

## Abstract

Large-scale neuronal networks and their complex distributed microcircuits are essential to generate perception, cognition, and behavior that emerge from patterns of spatiotemporal neuronal activity. These dynamic patterns emerging from functional groups of interconnected neuronal ensembles facilitate precise computations for processing and coding multiscale neural information, thereby driving higher brain functions. To probe the computational principles of neural dynamics underlying this complexity and investigate the multiscale impact of biological processes in health and disease, large-scale simultaneous recordings have become instrumental. Here, a high-density microelectrode array (HD-MEA) is employed to study two modalities of neural dynamics - hippocampal and olfactory bulb circuits from *ex-vivo* mouse brain slices and neuronal networks from *in-vitro* cell cultures of human induced pluripotent stem cells (iPSCs). The HD-MEA platform, with 4096 microelectrodes, enables non-invasive, multi-site, label-free recordings of extracellular firing patterns from thousands of neuronal ensembles simultaneously at high spatiotemporal resolution. This approach allows the characterization of several electrophysiological network-wide features, including single-/multi-unit spiking activity patterns and local field potential oscillations. To scrutinize these multidimensional neural data, we have developed several computational tools incorporating machine learning algorithms, automatic event detection and classification, graph theory, and other advanced analyses. By supplementing these computational pipelines with this platform, we provide a methodology for studying the large, multiscale, and multimodal dynamics from cell assemblies to networks. This can potentially advance our understanding of complex brain functions and cognitive processes in health and disease. Commitment to open science and insights into large-scale computational neural dynamics could

enhance brain-inspired modeling, neuromorphic computing, and neural learning algorithms. Furthermore, understanding the underlying mechanisms of impaired large-scale neural computations and their interconnected microcircuit dynamics could lead to the identification of specific biomarkers, paving the way for more accurate diagnostic tools and targeted therapies for neurological disorders.

## Introduction

Neuronal ensembles, often termed cell assemblies, are pivotal in neural coding, facilitating intricate computations for processing multiscale neural information<sup>1,2,3</sup>. These ensembles underpin the formation of expansive neuronal networks and their nuanced microcircuits<sup>4</sup>. Such networks and their oscillatory patterns drive advanced brain functions, including perception and cognition. While extensive research has explored specific neuronal types and synaptic pathways, a deeper understanding of how neurons collaboratively form cell assemblies and influence spatiotemporal information processing across circuits and networks remains elusive<sup>5</sup>.

Acute, *ex-vivo* brain slices are pivotal electrophysiological tools for studying intact neural circuits, offering a controlled setting to probe oscillatory activity patterns of neural function, synaptic transmission, and connectivity, with implications in pharmacological testing and disease modeling<sup>6,7,8</sup>. This study protocol highlights two key brain circuits - the hippocampal-cortical (HC) involved in learning and memory processes<sup>9,10</sup>, and the olfactory bulb (OB) responsible for odor discrimination<sup>11,12,13</sup>. In these two regions, new functional neurons are continuously generated by adult neurogenesis throughout life in mammalian brains<sup>14</sup>. Both circuits demonstrate multidimensional dynamic neural activity patterns and inherent plasticity that participate in rewiring the existing neural network and facilitate alternative information processing strategies when required<sup>15,16</sup>.

Acute, *ex-vivo* brain slice models are indispensable for delving into brain functionality and understanding disease mechanisms at the microcircuit level. However, *in-vitro* cell cultures derived from human induced pluripotent stem cells (iPSCs) neuronal networks offer a promising avenue of translational research, seamlessly connecting findings from animal experiments to potential human clinical treatment<sup>17,18</sup>. These human-centric *in-vitro* assays serve as a reliable platform for assessing pharmacological toxicity, enabling precise drug screening, and furthering research into innovative cell-based therapeutic strategies<sup>19,20</sup>. Recognizing the pivotal role of the iPSC neuronal model, we have dedicated the third module of this protocol study to thoroughly investigate the functional characteristics of its derived networks and to fine-tune the associated cell culture protocols.

These electrogenic neural modules have been commonly studied using techniques like calcium ( $\text{Ca}^{2+}$  imaging), patch-clamp recordings, and low-density microelectrode arrays (LD-MEA). While  $\text{Ca}^{2+}$  imaging offers single-cell activity mapping, it is a cell-labeling-based method hindered by its low temporal resolution and challenges in long-term recordings. LD-MEAs lack spatial precision, while patch-clamp, being an invasive single-site technique and laborious, often yields a low success rate<sup>21,22,23</sup>. To address these challenges and effectively probe network-wide activity, large-

scale simultaneous neural recordings have emerged as a pivotal approach for understanding the computational principles of neural dynamics underlying brain complexity and their implications in health and disease<sup>24,25</sup>.

In this JoVE protocol, we demonstrate a large-scale neural recording method based on the high-density MEA (HD-MEA) for capturing spatiotemporal neuronal activity across various brain modalities, including hippocampal and olfactory bulb circuits from *ex-vivo* mouse brain acute slices (**Figures 1A-C**) and *in-vitro* human iPSC-derived neuronal networks (**Figures 1D-E**), previously reported by our group and other colleagues<sup>26,27,28,29,30,31,32,33,34,35</sup>. The HD-MEA, built on complementary-metal-oxide-semiconductor (CMOS) technology, boasts on-chip circuitry and amplification, allowing sub-millisecond recordings across a 7mm<sup>2</sup> array size<sup>36</sup>. This non-invasive approach captures multi-site, label-free extracellular firing patterns from thousands of neuronal ensembles simultaneously using 4096 microelectrodes at a high spatiotemporal resolution, revealing the intricate dynamics of local field potentials (LFPs) and multiunit spiking activity (MUA)<sup>26,29</sup>.

Given the vastness of the data generated by this methodology, a sophisticated analytical framework is essential, yet poses challenges<sup>37</sup>. We have developed computational tools that encompass automatic event detection, classification, graph theory, machine learning, and other advanced techniques (**Figure 1F**)<sup>26,29,38,39</sup>. Integrating the HD-MEA with these analytical tools, a holistic approach is devised to probe the intricate dynamics from individual cell assemblies to broader neural networks across diverse neural modalities. This combined approach deepens our grasp of the computational dynamics in normal brain functions and offers insights into anomalies

present in pathological conditions<sup>28</sup>. Moreover, insights from this approach can propel advancements in brain-inspired modeling, neuromorphic computing, and neural learning algorithms. Ultimately, this method holds promise in uncovering the core mechanisms behind neural network disruptions, potentially identifying biomarkers, and guiding the creation of precise diagnostic tools and targeted treatments for neurological conditions.

## Protocol

All experiments were performed in accordance with the applicable European and national regulations (Tierschutzgesetz) and were approved by the local authority (Landesdirektion Sachsen; 25-5131/476/14).

### 1. *Ex-vivo* brain slices from hippocampal-cortical and olfactory bulb circuits on HD-MEA

1. Preparation of experimental cutting and recording solutions (**Figure 2A**)
  1. On the experimental day, prepare 0.5 L of high-sucrose cutting solution and 1 L of artificial cerebrospinal fluid (aCSF) recording solution (**Table 1A,B**).
  1. Add all solid chemicals to a dry volumetric flask, then fill part of the way with double distilled (dd) water.
  2. Add MgCl<sub>2</sub> and CaCl<sub>2</sub> from 1 M stock solutions, then fill the remainder with dd water. Begin constantly stirring with a magnetic stirrer until visible solids have dissolved ~5 min.
2. Use a freezing point osmometer to validate the osmolarity between 350-360 mOsm for the high-

sucrose cutting solution and 315-325 mOsm for the aCSF recording solution.

3. Use a pH meter to validate the pH between 7.3-7.4 for the high-sucrose cutting solution and 7.25-7.35 for the aCSF recording solution. Begin continuously bubbling with 95% O<sub>2</sub> and 5% CO<sub>2</sub>.
4. Place the high-sucrose cutting solution on ice for at least 30 minutes prior to slicing and begin continuously bubbling with 95% O<sub>2</sub> and 5% CO<sub>2</sub>.
5. After 10 min of carbogenation, fill a 50 mL beaker with 30 mL cutting solution and store it in the freezer (-20 °C) for 20-30 min or until partially frozen.

**NOTE:** All solutions should be prepared fresh for each experiment. The dd water used here is autoclaved ultrapure water stored at room temperature (RT). The amount of solution prepared should be tailored to the specific study question.

## 2. Preparation of brain slice workspace areas (**Figure 2A**)

1. Bring the animal into the experimental room.
 

**NOTE:** In this protocol, C57BL/J6 female mice aged 8-16 weeks were used as previously described<sup>26,29,32</sup>. The animal should be allowed to acclimate for at least 30 min after transport. Long-distance transfers (i.e., inter-institute) should be avoided on the same day as the experiment. The age, sex, and strain of the animal have to be determined based on the specific study question.
2. While the animal is acclimating and the high-sucrose solution is cooling down, place the required tools in each designated workspace (see **Table of Materials**).

3. Prepare **brain slice recovery and maintenance workspace**. Fill the slice recovery chamber with carbogenated aCSF recording solution and place the chamber in the water bath set to 32 °C. Maintain continuous carbogenation throughout the experiment.
4. Prepare **brain slice preparation workspace**. Setup the vibratome - place the blade in the vibratome blade holder and calibrate the vibratome to the correct settings (blade travel speed: 0.20 mm/s, height amplitude: 95 μm, blade angle: 45°). Fill the vibratome ice tray with ice and the buffer tray with a high-sucrose cutting solution and begin carbogenating the solution in the buffer tray.
5. Prepare the **brain preparation workspace**. Fill the 150 mm glass Petri dish with ice and place a 90 mm plastic culture dish with filter paper inside. Fill the plastic culture dish with a high-sucrose cutting solution and begin carbogenating. Add a drop of super glue to the chilled specimen plate and attach the agarose mold.
 

**NOTE:** Agarose mold is prepared at least the day before with 3% agarose in water in a custom mouse brain mold.
6. Lastly, prepare the **brain extraction workspace**. Cover aluminum foil with tissue paper, retrieve a 50 mL beaker containing high-sucrose cutting solution slush, and add isoflurane to the anesthesia chamber.
 

**NOTE:** Anesthesia will be added to the anesthesia chamber ~1 min prior to animal placement. A 50 mL beaker with 30 mL of high-sucrose cutting solution

slush will be removed from -20 °C freezer ~2 min before decapitation.

### 3. Extraction and slicing of mouse brain

**NOTE:** This entire procedure should be performed as quickly as possible to avoid a lack of oxygenation to the brain. Brain removal should only take 1-2 min from decapitation to immersion in the high-sucrose cutting solution slush.

1. Anesthetize the animal with the appropriate dosage of isoflurane (0.5 mL/1 L anesthesia chamber). Determine the depth of anesthesia through a paw pinch; confirm the lack of paw withdrawal reflex before proceeding.
2. Transfer the animal to the tissue paper in the brain extraction workspace and decapitate it with surgical scissors.
3. Insert iris scissors into the brain stem and keep the bottom scissors flush with the calvaria. Cut along the sagittal suture until the coronal suture is reached. Place iris scissors in eye sockets and cut through the metopic suture. Use curved forceps to move the sides of the calvaria down, exposing the whole brain.  
**NOTE:** Be careful with both the iris scissors and forceps to not puncture the brain while cutting through the sutures.
4. Slide the brain with the blunt edge of the curved forceps into the 50 mL beaker with 30 mL of high-sucrose cutting solution slush. Let it remain for 1 min.
5. Transfer the brain to the 90 mm plastic culture dish with chilled carbogenated cutting solution in the brain preparation workspace. Orient the brain for positioning in the agarose mold.

6. Add a small dot of super glue to the rostral end of the agarose mold. Place the brain in the mold with the spatula. Ensure that the brain is placed with the dorsal side down for horizontal slicing.

**NOTE:** The location of glue in the mold will change depending on the region of interest (ROI). For hippocampal-cortical (HC) and olfactory bulb (OB) slices, ensure that the OB is stabilized and the sides of the brain remain free from glue. Too much glue will affect slicing quality and cause tears during vibratome slicing.

7. Move the specimen plate into the buffer tray, move the blade into position with the correct angle, and increase the buffer tray height to bring the blade as close as possible to the brain.
8. Slice at 0.20 mm/s speed 300 µm intervals of HC and OB tissues, then collect them after each slicing round with a glass Pasteur pipette.
9. Leave the slices in the aCSF-filled recovery chamber in a 32 °C water bath for 45 min, followed by 1 h at RT. Ensure slices do not overlap and are fully exposed to the carbogenated solution.

**NOTE:** Be sure to maintain continuous carbogenation of all solutions and any chambers mentioned containing the solution. A pressure regulator may be used to sustain consistent carbogenation.

## 2. *In-vitro* human iPSC-based neuronal network on HD-MEA

**NOTE:** All iPSC neurons used in this study are commercially obtained (see **Table of Materials**). These human cells

differentiated from stable iPSC cell lines that were derived from human peripheral blood or fibroblasts.

1. Coating of HD-MEA chips for *in-vitro* human iPSC cell cultures (**Figure 2B**)

1. Place the HD-MEA chip on the acquisition recording platform, fill the reservoir with PBS, and test the chip prior to coating. Start Brainwave software. Select **File > New Recording Session**. Set the recording parameters to have a **Recording Frequency** of 50 Hz and a **Sampling Frequency** of 18 kHz/electrode. Change the **Amplifier Offset** to calibrate the chip. See **Table 2** for troubleshooting tips.

**NOTE:** The recording frequency and sampling frequency parameters will depend on data type and individual system requirements.

2. Sterilize and pre-condition HD-MEAs.

1. Under the hood, wipe the chip and the glass ring with tissue moistened with 96% ethanol (EtOH), then place each device into a sterile 100 mm x 20 mm Petri dish and fill the MEA reservoir with 70% EtOH for 20 min.
2. Aspirate the EtOH and wash the reservoir with sterile, filtered dd-water 3 times. Add 1 mL of pre-conditioning media and incubate overnight at 37 °C and 5% CO<sub>2</sub>.

**NOTE:** Pre-conditioning media needs to be a salt-based solution to make the HD-MEA surface more hydrophilic. This can include previously prepared BrainPhys (BP) complete media (not >3 months old) (**Tables 1C**).

3. Coat HD-MEAs. The next day, aspirate pre-conditioning media. Add 1 mL of 0.1 mg/mL poly-

dl-ornithine (PDLO) to coat the entire active area. Incubate at 37 °C overnight in an incubator.

4. Prepare and warm media to RT. The protocols here exploit functional human iPSC neurons from two commercial sources; thus, media components vary for each supplier. One protocol is described in (**Tables 1C, D**).

5. Aspirate PDLO, wash 3 times with dd-water and let the chips dry under the hood for 10 min.

6. Fill a 35 mm x 10 mm Petri dish with sterile, filtered dd-water and place it beside the chip to maintain proper humidity and avoid evaporation of the seeded cells in the next steps.

2. Plating and maintenance of human iPSC neurons in HD-MEAs (**Figure 2B**)

1. Thaw and dilute cells to desired cells per microliter concentration (i.e., 1000 cells/μL to obtain 50,000 cell density in a 50 μL drop on the HD-MEA) (**Table 1C**).

2. Pipette the cell suspension on the surface of the chip active area using high laminin dotting media (**Table 1D**).

3. Incubate at 37 °C with 5% CO<sub>2</sub> for 45-60 min.

4. Gently fill 2 mL of media in the HD-MEA reservoir (**Table 1C**).

5. Perform 100% media change on day 1 (DIV1) post-seeding using RT media (**Table 1C**). Change 50% of the media every 3-4 days. Keep HD-MEAs incubated at 37 °C with 5% CO<sub>2</sub> throughout the experiment.

**NOTE:** Pipette gently to avoid dislodging the cells. Check the color of the media for any contamination.

The interval and amount of media change can be determined by individual study questions or cell needs/specifications.

- Optional: Check the progress of cell culture growth between DIV4-DIV8 under an upright differential interference contrast (DIC) microscope after cleaning the stage with >70% EtOH.

### 3. *Ex-vivo* and *in-vitro* large-scale neural recordings with HD-MEAs

#### 1. Preparation of brain slice recording workspace (Figure 2A)

- While brain slices are recovering, place the required tools in each designated workspace (see **Table of Materials**).

**NOTE:** The main system setup must be optimized and tested well before the brain slice experimental day. The perfusion system (inlet lines, pump outlet lines, tubing, and grounding) needs to be tested with PBS or aCSF and an HD-MEA on the recording platform to ensure a clean signal, increased signal-to-noise ratio, and lack of perfusion noise.

- Coat the HD-MEA chip with 0.1 mg/mL of PDLO to enhance tissue-chip coupling and incubate at 37 °C for 20 min.
- During chip incubation, fill the gravity-based perfusion system and lines with recording aCSF. Ensure continuous carbogenation of the perfusion system. Set a flow rate of 4.5 mL/min and a temperature of 37 °C.
- Place the HD-MEA chip on the acquisition recording platform, fill the reservoir with aCSF, test the

perfusion system, and troubleshoot any remaining system noise.

- Start Brainwave software. Select **File > New Recording Session**. Set the recording parameters to have a **Recording Frequency** of 1 Hz and a **Sampling Frequency** of 14 kHz/electrode. Change the **Amplifier Offset** to calibrate the chip. See **Table 2** for troubleshooting tips.

**NOTE:** The recording frequency and sampling frequency parameters will depend on data type and individual system requirements.

- Ensure the recording area is dark through a room lighting system or a shaded cage on the optical table.
- Align the stereomicroscope with the HD-MEA chip reservoir and active area for image acquisition.
- Place the anchor in the chip reservoir to equilibrate.
 

**NOTE:** Anchor is a custom-made platinum harp with minimal wires to promote oxygenation; however, some commercial ones are available.
- Add pharmacological compounds to the appropriate perfusion tubes.
 

**NOTE:** In this protocol, both spontaneous and 100 μM 4-aminopyridine (4-AP) pharmacologically induced recordings were obtained as previously described. Pharmacological compounds can be tailored to the specific study question.
- In the brain slice preparation workspace, place a new 90 mm plastic culture dish in a 150 mm glass Petri dish. Add aCSF and begin carbogenating.

#### 2. Circuit-wide recordings from HC and OB slices using HD-MEAs

**NOTE:** Slice coupling should be performed as quickly as possible to avoid a lack of oxygenation to the slice. Coupling should only take ~1 min from the initial placement of the microdissected slice on the chip active area to the final perfusion system startup.

1. Remove the slice from the brain slice recovery chamber with a glass pipette and place it in a 90 mm plastic culture dish with continuous carbogenation. Using a microdissection tool, isolate the HC or OB from the surrounding brain slice tissue.
2. Move the isolated HC or OB acute slices with a glass pipette into the HD-MEA reservoir. Gently align the slice on the MEA active area with a fine brush. Suck all solutions from the HD-MEA chip well with an aspiration system.
3. Place the anchor gently on top of the slice using forceps.
 

**NOTE:** The anchor should be placed without slice movement to avoid the loss of coupling.
4. Gently add solution to the chip reservoir and start the perfusion system.
 

**NOTE:** Ensure laminar flow from the perfusion inlet and pump outlet for optimal recording parameters.
5. Ensure the recording area is adequately dimmed through the room lighting system or with a shaded cage on an optical table setup.
6. Allow the slice to acclimate for 10 min before beginning recordings or additional pharmacological modulation.
7. Start Brainwave software. Select **File > New Recording Session**. Set the recording parameters to have a **Recording Frequency** of 1 Hz and a

**Sampling Frequency** of 14 kHz/electrode. Change the **Amplifier Offset** to calibrate the chip.

**NOTE:** As denoted earlier in section 3.1.4.1, while performing system tests, make sure to apply these same recording parameters.

8. Press **Record** to begin the acquisition with the preset experimental conditions.
  9. Immediately following the final recording, capture light imaging of the acute brain slice. Move the slice back to the slice recovery chamber, remove any organic material coupled to the chip with a brush, and continue with the next slice. Clean the HD-MEAs as described in section 3.4.
3. Preparation of human iPSC recording workspace and network-wide recordings on HD-MEA (**Figure 2B**)
 

**NOTE:** Change media either the day before recording or immediately following human iPSC recording (**Table 1C**). In studies using the functional neurons, media was changed every 4 days, and on 4, 8, 16, and 24 DIV media is changed immediately following iPSC recordings.

    1. Ensure a sterile work environment by cleaning the HD-MEA acquisition platform with >70% EtOH.
    2. Gently place a polydimethylsiloxane (PDMS)-base cap with reference on the HD-MEA ring under the hood. Move the HD-MEA chip to the iPSC recording workspace and attach the HD-MEA chip to the acquisition platform.
    3. Ensure the recording area is adequately dimmed through a room lighting system or a shaded cage on an optical table.
    4. Allow the HD-MEA chip to equilibrate for 10 min prior to beginning recordings or additional pharmacological modulation.

5. Start Brainwave software. Select **File > New Recording Session**. Set the recording parameters to have a **Recording Frequency** of 50 Hz and a **Sampling Frequency** of 18 kHz/electrode. Change the **Amplifier Offset** to calibrate the chip.

**NOTE:** As denoted earlier in section 2.1.1, while performing a system test prior to coating and plating, make sure to apply these same recording parameters.

6. **Record** the spontaneous firing activity or pharmacologically induced responses from the human iPSC network on each day of the experimental plan (i.e., 4, 8, 16, 24 DIVs).

**NOTE:** Do not let the chip remain outside the incubator for >30 min to maintain stable temperature and humidity and prevent any temperature shock to cells.

7. Incubate HD-MEAs at 37 °C with 5% CO<sub>2</sub> over the course of the experiment.

8. Following experiment completion, fix the neuronal network on chips and stain for further optical imaging or clean the HD-MEAs directly, as described in step 3.4.

#### 4. Cleaning of HD-MEA chips

1. After the experiment, discard the solution according to proper waste disposal and rinse with dd-water.

2. Add the detergent of choice, clean the active area and entire reservoir with a Q-tip, and discard the detergent. Refill with detergent, incubate for 20 min, then discard detergent.

3. Thoroughly rinse with laboratory-grade water. Then, rinse 3-4 times with dd-water.

4. Use air pressure to dry the HD-MEA chip thoroughly.

#### 4. Analysis of large-scale neural recordings from HD-MEAs

**NOTE:** While step 4.1 is Brainwave software specific, step 4.2 can be modified based on each user's commercially available HD-MEA device type.

##### 1. Raw data preprocessing and event detection

1. Open a recorded raw data file (.brw) in Brainwave software. Select **Analysis > LFP Detection** or **Spike Detection**.

**NOTE:** LFP Detection employs IIR filtering with a low pass 4<sup>th</sup> order Butterworth filter (1-100 Hz). Hard threshold algorithms include a high threshold of 150 μV, a low threshold of -150 μV, an energy window between 70-120 ms, a refractory period of 10 ms, and a maximum event duration of 1 s. Single and MUA Spike Detection employs IIR filtering with a high pass 4<sup>th</sup> order Butterworth filter (300-3500 Hz). A PTSD algorithm is applied with a standard deviation factor of 8, a peak lifetime period of 2 ms, and a refractory period of 1 ms.

2. For HC and OB circuit recordings, add the **Advanced Workspace** option in the detected event file (.bxr) to import the structural light image captured from the stereomicroscope. When examining large-scale HC circuitry, create structural layers containing the dentate gyrus (DG), hilus, Cornu Ammonis 1 (CA1), Cornu Ammonis 3 (CA3), entorhinal cortex (EC), and perirhinal cortex (PC). When examining large-scale OB circuitry, create structural layers containing the olfactory nerve layer (ONL), glomerular layer (GL), external plexiform layer

(EPL), mitral cell layer (MCL), and granule cell layer (GCL). Consider the EPL and the MCL as the projection layer (PL), including the olfactory cortex (OCx).

## 2. Data processing with a custom Python computational pipeline

### 1. Denoising

1. Read .bxx file using a custom-written Python script<sup>26, 29, 32</sup> and h5py 3.6.0 python package.
2. Extract spike trains pertaining to the iPSC network recordings and LFP event trains pertaining to the HC and OB brain slice circuit recordings.
3. Characterize events with a total number of active electrodes less than 0.1% or 10% of the average active electrodes per average event or detected events falling outside a statistically reasonable firing rate range as random events and remove them. Additionally, apply amplitude and event duration threshold values.

**NOTE:** For the firing rate range, 0.1-15 spikes/s and 0.1-60 LFP events/min are considered. These are example rate threshold values used for the analyzed datasets. The rate, amplitude, and duration thresholds will depend on individual data.

4. Save the resultant event train data with the accompanying spatiotemporal information in .npy file format.

### 2. Rastergrams

1. Read filtered event .npy and .bxx files and generate a raster plot using the Matplotlib

pyplot function ([https://matplotlib.org/3.5.3/api/\\_as\\_gen/matplotlib.pyplot.html](https://matplotlib.org/3.5.3/api/_as_gen/matplotlib.pyplot.html)).

2. Additionally, for brain slice recordings with layer specificity, sort and group the electrode IDs based on the layers produced in step 4.1.2.

### 3. Mean firing activity

1. Process the time series data from the .bxx file, calculating each electrode's average firing rate (number of events/recording time).
2. Construct a data matrix where the rows and columns represent the coordinates of electrodes in the HD-MEA 64 x 64 array, where each matrix value signifies the mean firing rate.
3. Employ a plotting library such as Matplotlib's imshow or Seaborn's heatmap functions in Python.
4. Employ the 'hot' color map here, creating an informative heatmap that visually encapsulates the spatial distribution of mean firing rates across the electrode array.

### 4. Representative waveform traces

1. Read time series data from the .brw file and generate a waveform trace using Matplotlib pyplot function. ([https://matplotlib.org/3.5.3/api/\\_as\\_gen/matplotlib.pyplot.html](https://matplotlib.org/3.5.3/api/_as_gen/matplotlib.pyplot.html)).
2. Input desired electrode ID, time bin, and frequency band for a representative waveform trace. Frequency bands defined in these analyses include low-frequency LFP oscillations (1-100 Hz) with bandpass filtered  $\delta$ ,  $\theta$ ,  $\beta$ , and  $\gamma$  frequency bands; sharp wave ripples (SWR) (140-220 Hz); and high-frequency single

and MUA (300-3500 Hz). The frequency bands  $\delta$ ,  $\theta$ ,  $\beta$ , and  $\gamma$  are 1-4 Hz, 5-12 Hz, 13-35 Hz, and 35-100 Hz respectively.

## 5. Power spectral density

1. Read time series data from the .brw file and compute the periodograms to discern the dominant frequencies underlying the oscillatory activity within each time series.
2. Construct pseudo-color spectrograms of the frequency-time dynamics.  
**NOTE:** Spectra are calculated using Welch's method by utilizing the Fast Fourier Transform of recorded LFPs to estimate spectral power density<sup>41</sup>.
3. Input desired electrode ID, time bin, and frequency band for a spectral density map. Frequency bands defined in these analyses include those described in step 4.2.4.

## 6. Functional connectivity

1. For brain slice circuit recordings, follow steps 4.2.6.2-4.2.6.4.
2. Read time series data from the .brw file and calculate the cross-covariance between pairs of active electrodes in the 64 x 64 array employing Pearson's correlation coefficient (PCC)<sup>42</sup>.
3. Fit a vector autoregressive model to the time series using Multivariate Granger causality to quantify the influence of one time series on another.
4. Apply directed transfer function (DTF) to assess directional information flow within the correlated links.

**NOTE:** Functional connectivity in the multilayered network is established by setting a correlation value threshold based on those over the mean and two standard deviations of all cross-covariance values<sup>43,44</sup>.

5. For iPSC recording, follow steps 4.2.6.6-4.2.6.8.
6. Read spiketrains data from the .bxx file and compute a 64x64 matrix of the PCC correlation coefficients between all combinations of binned spike trains using spike\_train\_correlation functions ([https://elephant.readthedocs.io/en/v0.7.0/reference/spike\\_train\\_correlation.html](https://elephant.readthedocs.io/en/v0.7.0/reference/spike_train_correlation.html)).  
**NOTE:** Functional connectivity in the multilayered network is established by setting a correlation value threshold based on those over the mean and two standard deviations of all cross-covariance values.
7. Furthermore, implement spatial-temporal filters (STF) and distance-dependent latency thresholds (DdLT) filtering procedures on the connectivity matrix to eliminate potential paired connections exceeding the maximum propagation velocity (set at 400 mm/s)<sup>45</sup>.
8. Extract negative peaks from resultant cross-correlation matrices with filtering and thresholding operations to identify the inhibitory connections using filtered and normalized cross-correlation histogram (FNCCH) algorithm<sup>45</sup>.
9. Transform each connectivity matrix into a dynamic graph (.gexf) file.

## 7. Network connectivity maps

1. Open **data laboratory** in Gephi program 9.2 version (<https://gephi.org>) for the dynamic graph to plot specific time bins.
2. Apply **Geo Layout** in the layout window for spatial mapping.
3. Place parameter constraints on **Degree Range** and **Edge Weight** for comparison.
4. Assign **Nodal Color, Edge Size, and Degree Size** for better visualization.

## Representative Results

### Multimodel spatiotemporal mapping and extraction of oscillatory firing features

To quantify network-wide LFP and spike events that emerged from dynamical neuronal ensembles, we investigated synchronous large-scale firing patterns in HC and OB circuits and human iPSC networks. Recorded brain slice circuits from step 3.2 and recorded iPSC networks from step 3.3 were analyzed according to steps 4.1-4.2 of the protocol. First, event detection and denoising were performed for all recorded datasets and regionally resolved according to circuit specifications. Next, topographical pseudo-color spatial mapping of mean large-scale LFP and spike firing patterns, rastergrams of detected events, and representative 5-s traces of filtered waveforms were plotted (**Figures 3A-I**). Topographical pseudo-color mapping of large-scale LFP and spike firing rate patterns were overlaid on the respective microscope-captured optical images of HC (**Figure 3A**), OB (**Figure 3B**), and human iPSC neuronal network (**Figure 3C**). This allows the investigation of individual circuit and network-based oscillatory patterns and responses. HC and OB rastergrams contain detected LFP event counts sorted over the DG, Hilus, CA3, CA1, EC, and PC layers of

the HC circuit and ONL, OCx, GL, PL, and GCL layers of the OB network over a 60-s time bin (**Figures 3D,E**). The human iPSC rastergram displays synchronous detected spike events of the interconnected cultured network over a 20 s time bin (**Figure 3G**). Next, 5s representative event traces from large-scale HD-MEA recording sites show a range of recorded oscillatory frequencies in the HC (i.e., selected electrode in CA3) (**Figure 3G**) and OB (i.e., selected electrode in GL) (**Figure 3H**) circuits and multiunit spike bursting activity in the human iPSC network from four selected active electrodes in the array (**Figure 3I**). These exemplary signals show biosignal signatures, including low-frequency LFP oscillations (1-100 Hz) with bandpass filtered  $\delta$ ,  $\theta$ ,  $\beta$ , and  $\gamma$  frequency bands; sharp wave ripples (SWR) (140-220 Hz); and high-frequency single and MUA (300-3500 Hz). Finally, power spectral density (PSD) analysis was employed to simultaneously quantify a specific oscillatory band's power magnitude in the interconnected HC and OB circuit recorded from HD-MEA (**Figures 3J,K**).

### Multimodal Network-wide Functional Connectome

To infer the large-scale connectivity of multilayered neural networks from simultaneously firing patterns of concurrently active neuronal ensembles, the cross-covariance between pairs of active electrodes in detected events was calculated according to step 4.2.6 of the protocol. Here, the correlation coefficient was sorted based on layers in the HC and OB circuit or unsorted in the iPSC network and then stored in a symmetric matrix. Functional connectomes of HC and OB circuitry were generated by applying Multivariate Granger causality and directed transfer function (DTF) to quantify the influence of one time series on another and assess the directional information flow within the correlated links in the distinct networks. Connectome mapping of HC (**Figure 4A**) and OB (**Figure 4B**) and network visualization were

performed using the Gephi program 9.2 version (<https://gephi.org>). Similar parameter constraints were placed on the functional links to compare the HC and OB brain slice circuits and illustrated 100 s of the functional connectivity of detected LFP events. Nodes are scaled according to degree strength with nodal color indicating layer and link color identifying the intra- and inter-layer connections. Functional connectomes of human iPSC networks were generated by applying

spatial-temporal filters (STF) and distance-dependent latency thresholds (DdLT) to enhance the selection of significant links and refine the identification of meaningful connections by applying filtered and normalized cross-correlation histogram (FNCCH) analysis. Connectome mapping of human iPSC networks on the entire HD-MEA chip (**Figure 4C**) visualization performed using Gephi. Nodal color indicates excitatory or inhibitory input, and link color identifies connections.

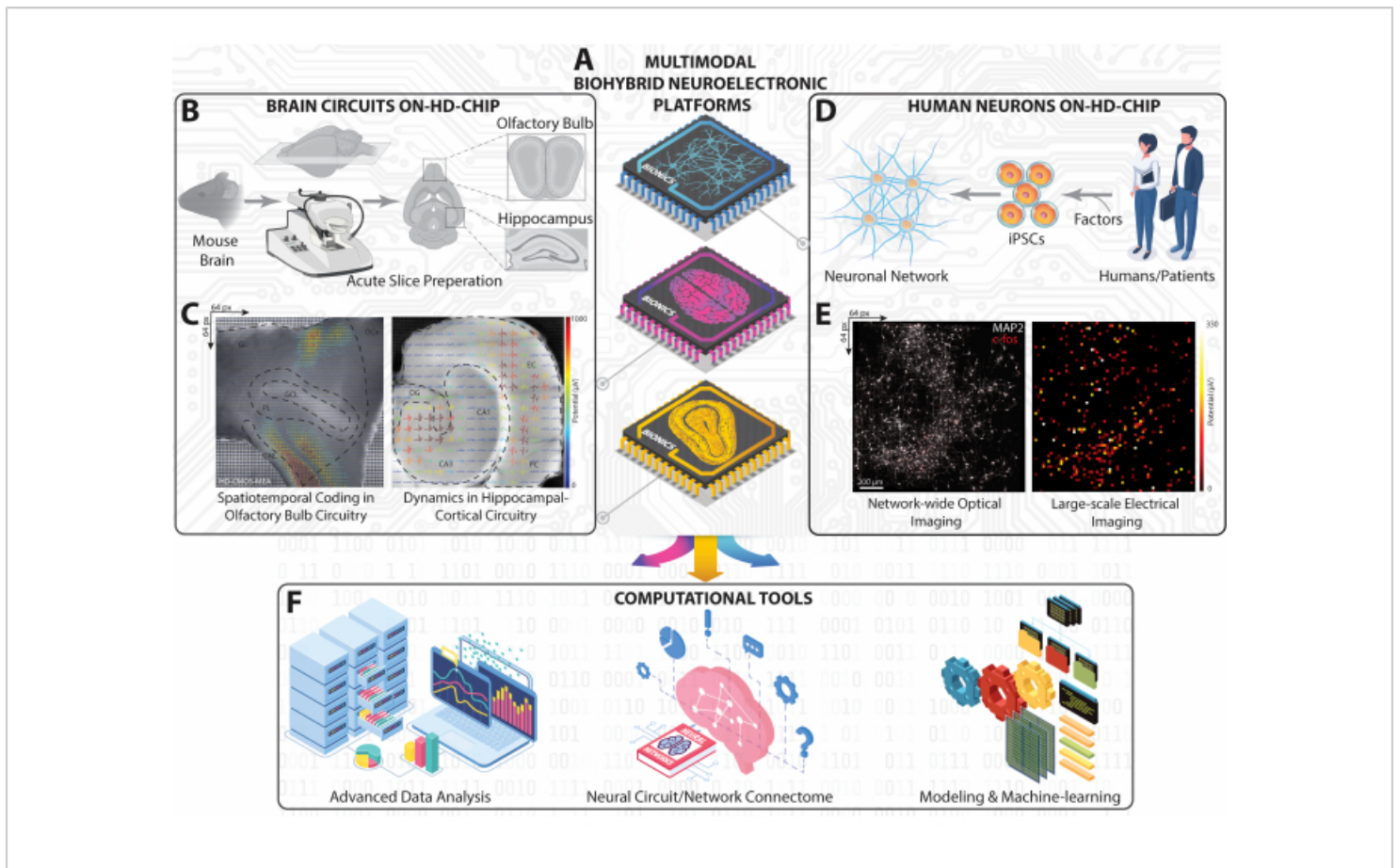
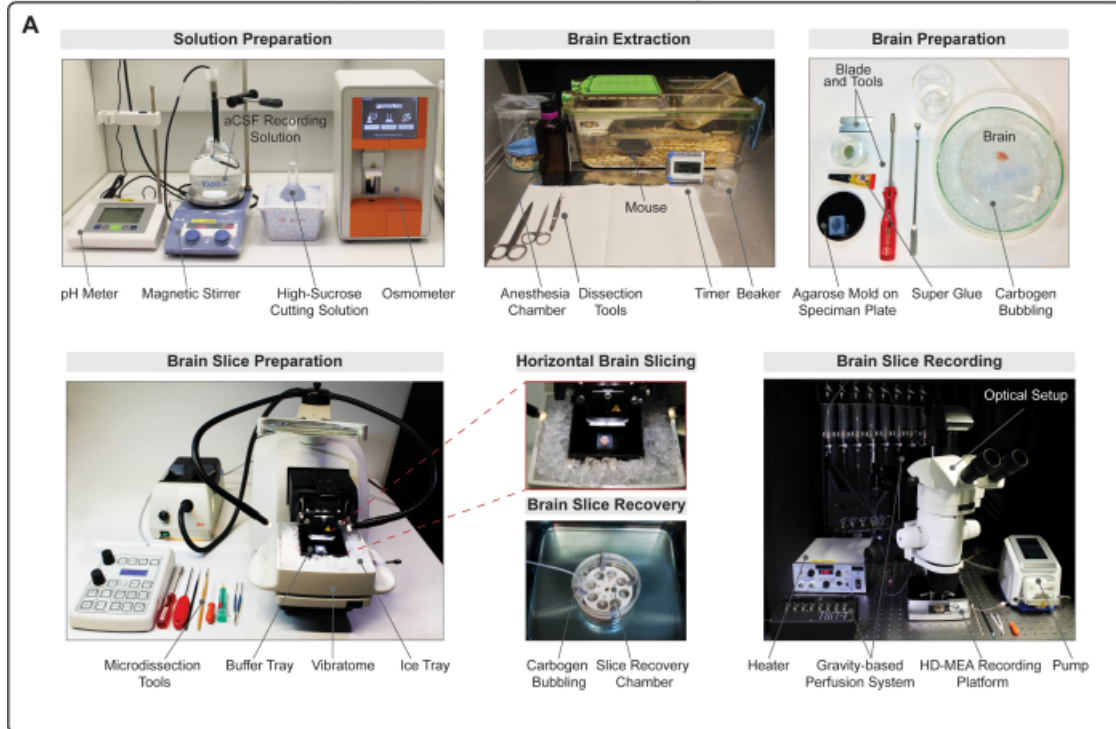


**Figure 1: Overview of the experimental and computational platform on large-scale HD-MEA.** (A) Isometric schematic representation of our multimodal biohybrid neuroelectronic platforms realized with CMOS-based HD-MEA to capture neural dynamics from HC, OB, and human iPSC neuronal circuits and networks. (B) Schematic workflow for mouse brain slicing and its workspace to obtain HC and OB slices. (C) Topographical representations of the large-scale firing patterns recorded simultaneously from the entire HC and OB slices superimposed with the extracted extracellular waveforms to the slice optical images. (D) Schematic representation of iPSC neuronal network obtained from humans. (E) Fluorescence micrographs

---

showing cellular c-fos and somatic/dendritic MAP-2 of the entire human neuronal network on HD-MEA chip (*left*) matched with the entire average firing activity map (*right*). (F) Computational framework including advanced data analysis, connectivity mapping, and AI-machine learning tools to analyze multidimensional neural data obtained from large-scale recordings on HD-MEAs. [Please click here to view a larger version of this figure.](#)

### Ex-vivo Brain Slices from Hippocampal-cortical and Olfactory Bulb Circuits on HD-MEA



### In-vitro Human iPSC-based Neuronal Network on HD-MEA

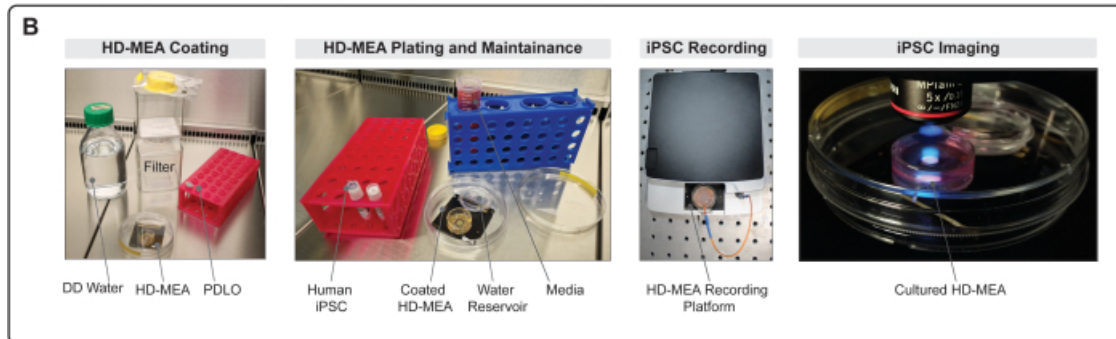


**Figure 2: Layouts for ex-vivo brain slice and in-vitro human iPSC culture preparation and recording workspaces. (A)** Schematic workflow illustrating the setup for preparing HC and OB slices, featuring the requisite tools and equipment in each workspace. **(B)** Schematic representation for human iPSC culture preparation, including the necessary tools and devices. A complete list of materials is included in steps 1.2.2, 2.1, 2.2, 3.1.1, 3.3, and the **Table of Materials**. [Please click here to view a larger version of this figure.](#)

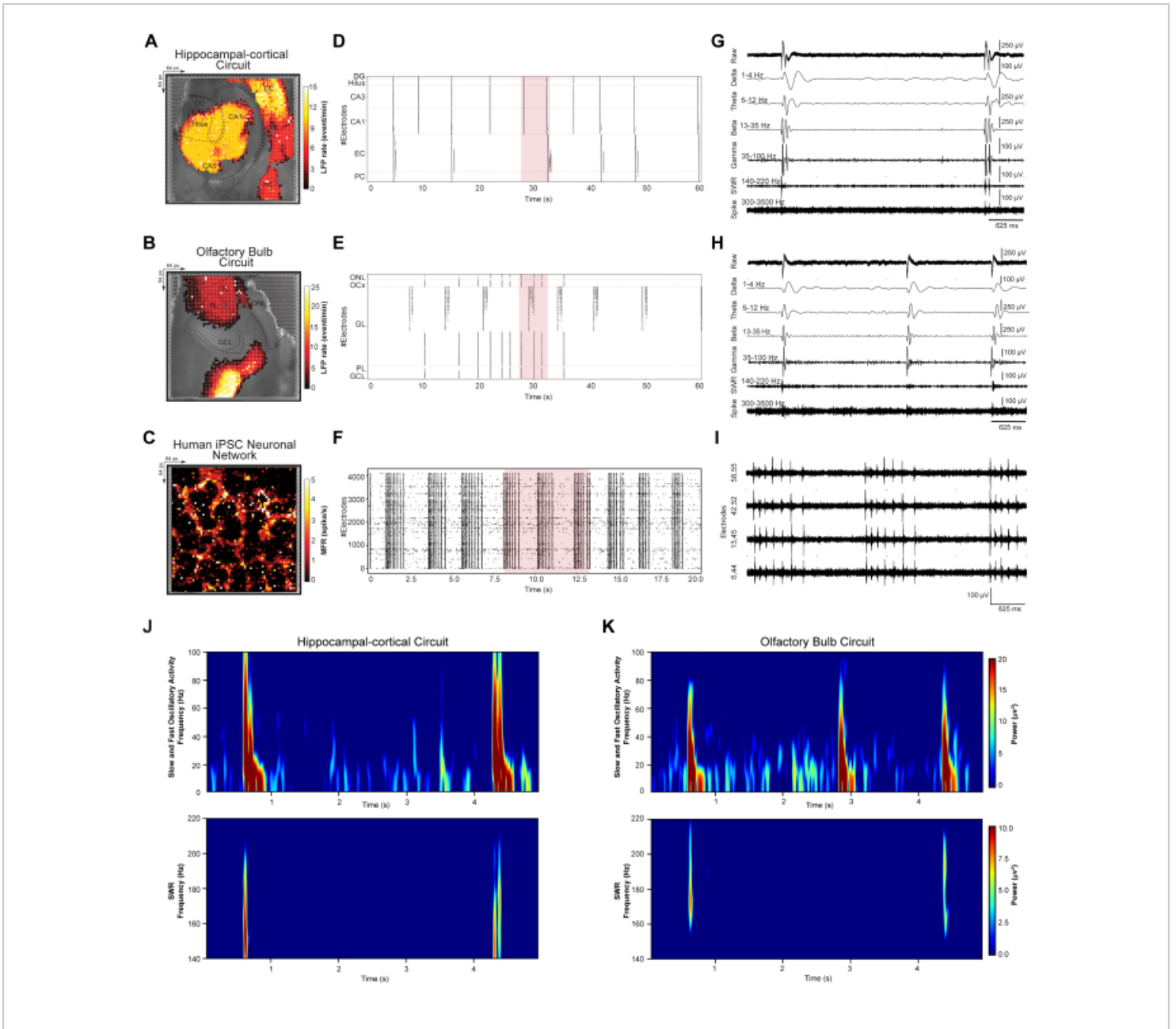


**Figure 3: Mapping and extracting spatiotemporal patterns of network dynamics. (A-C)** Mean LFP and spike rate spatial maps, computed over five-minute recordings, superimposed on the microscope light image. **(D-F)** Raster plots depicting detected, denoised LFP events in a 60-second data subsample and spikes in a 20-second data subsample. **(G-I)** Representative waveform trace extraction from a 5-second segment of the raster plot data subsample (highlighted red in the raster plot), displayed as raw LFP oscillatory bands (1-100 Hz);  $\delta$  (1-4 Hz),  $\theta$  (5-12 Hz),  $\beta$  (13-35 Hz), and  $\gamma$  (35-100 Hz) frequency bands; SWR (140-220 Hz); and high-frequency single and MUA spiking (300-3500 Hz). **(J,K)** Power spectral

density maps of fast and slow oscillatory LFPs (1-100 Hz) and SWR (140-220 Hz). [Please click here to view a larger version of this figure.](#)

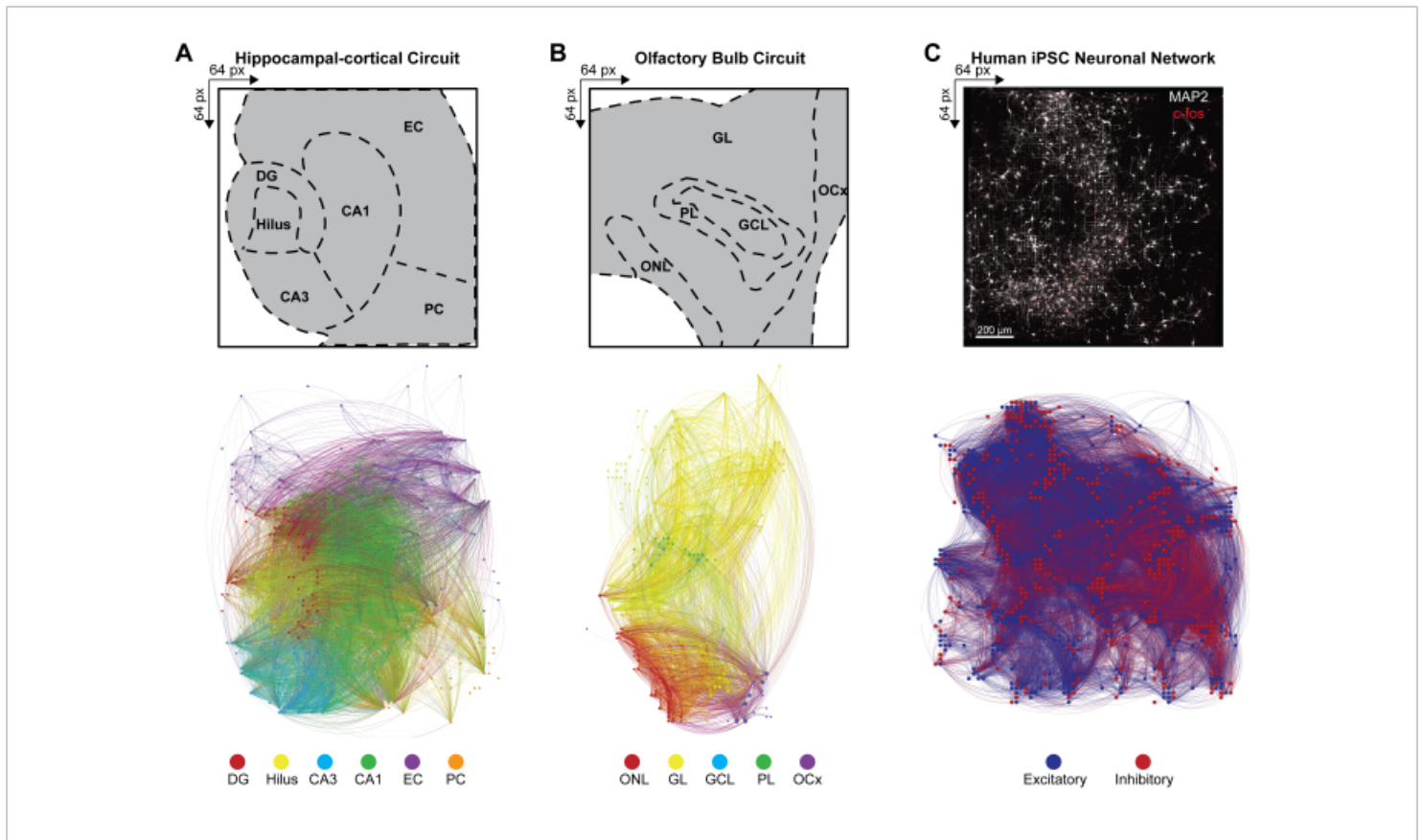


**Figure 4: Organization of multimodal network-wide functional connectomes.** (A-C) Gephi maps illustrating nodal functional connectivity, where nodes correspond to one of the example color bar legends (*below*), while the links (or edges) are shaded to match the connecting nodes. Example legends for (A) HC, (B) OB, and (C) iPSC layers are displayed on a 64 x 64 array. HC and OB layers are plotted over a 100-s time bin to effectively reduce the number of visible nodes and links for visualization purposes. [Please click here to view a larger version of this figure.](#)

**Table 1: Solutions for brain slice preparation and media for iPSC neuronal cultures.** (A) High-sucrose cutting solution for *ex-vivo* brain slice preparation. (B) aCSF recording solution for *ex-vivo* brain slice preparation and recording. (C-D) Human neuronal iPSC Media Protocol, where (C) is BrainPhys complete media used for cell thawing, HD-MEA chip coating, and cultured HD-MEA maintenance,

and (D) the dotting media used for HD-MEA cell plating. [Please click here to download this Table.](#)

**Table 2: Troubleshooting common HD-MEA recording acquisition issues.** A list of common problems, their potential causes, and troubleshooting solutions related to HD-MEA chips, recording platform, system noise, and software. [Please click here to download this Table.](#)

## Discussion

The intricate dynamics of spatiotemporal neuronal activity, emerging from interconnected neuronal ensembles, have long been a subject of intrigue in neuroscience. Traditional methodologies, such as patch-clamp, standard MEA, and  $\text{Ca}^{2+}$  imaging, have provided valuable insights into brain complexity. However, they often fall short in capturing the comprehensive network-wide computational dynamics<sup>21,22,23</sup>. The technical protocol of the HD-MEA platform, as detailed in this JoVE study, represents a significant leap forward, offering a panoramic view of neural dynamics across diverse modalities, from cell assemblies to expansive networks (i.e., acute, *ex-vivo* mouse brain slices and *in-vitro* human iPSC networks)<sup>26,29,30,32</sup>.

Acute, *ex-vivo* mouse brain slices have been a foundational tool in neuronal research, facilitating molecular and circuit-level investigations<sup>6,7</sup>. However, the challenge of maintaining tissue viability has been a persistent bottleneck. The protocol delineated in this study introduces critical modifications to optimize the quality and longevity of these slices to exploit their benefits on the HD-MEA platform. This protocol underscores the importance of - i) Achieving slice uniformity, for which the use of a vibratome is preferred over a tissue chopper due to its precision and minimized tissue damage, despite the trade-off of longer slicing times. ii) Ensuring constant carbogenation throughout the process, from extraction to recording, to maintain tissue viability. iii) Regulating temperature and allowing adequate recovery time before recording. iv) Utilizing an agarose block or mold to stabilize the brain, prevent tearing, and minimize glue contact. v) Maintaining optimal flow rates of carbogenated aCSF within the HD-MEA reservoir to ensure slice health while avoiding issues like decoupling, noise, and drift (**Table 2**).

For both mouse brain slices and human iPSC preparations, enhancing electrode-tissue interface coupling is paramount<sup>30,46,47</sup>. Our protocol underscores the importance of utilizing the adhesion-promoting molecule Poly-dl-ornithine (PDLO). This molecule not only augments the surface area for detecting electrical signals but also boosts electrical conductivity<sup>46</sup>. By doing so, it promotes cellular adhesion, growth, and the development of functional network properties. Such optimization plays a pivotal role in enhancing the efficacy of the HD-MEA platform. This, in turn, ensures accurate and consistent analysis of microscale *ex-vivo* and *in-vitro* connectomes and their spatiotemporal firing sequences. Notably, PDLO has been shown to outperform other substrates like polyethyleneimine (PEI) and poly-l-ornithine (PLO) in promoting spontaneous firing activity and responsiveness to electrical stimuli in neuronal cultures. Additionally, PDLO has been used for surface functionalization on the HD-MEA and shown to enhance the electrode-slice coupling interface and increase the signal-to-noise ratio in both OB and HC slices<sup>26,29</sup>. The addition of a custom-built platinum anchor further augments the electrode-slice interface coupling, leading to recordings with a higher signal-to-noise ratio.

The utilization of HD-MEA for both *ex-vivo* mouse brain slices and *in-vitro* human iPSC networks introduces a method adept at exploring extensive, multiscale, and multimodal dynamics. This innovative approach, however, brings forth considerable challenges, especially in data management<sup>48,49,50,51</sup>. A single HD-MEA recording acquired at 18 kHz/electrode sampling frequency generates a staggering 155 MB/s of data. The data volume escalates rapidly when factoring in multiple slices, diverse pharmacological conditions, or prolonged recording periods. Such an influx of information calls for robust storage infrastructures and advanced computational

tools for streamlined processing. The ability of the HD-MEA platform to simultaneously gather data from thousands of neuronal ensembles is both a boon and a hurdle. It provides supreme insights into the computational dynamics of brain functions, yet it also necessitates a refined analytical framework. In this JoVE protocol, we have provided examples of computational strategies, including large-scale event detection, classification, graph theory, frequency analysis, and machine learning. These methods underscore the intensive efforts made to tackle the challenges of analyzing complex neural data. Nonetheless, there is still considerable room for the development of more advanced computational tools to analyze these multidimensional neural datasets. Armed with the appropriate tools and methodologies, the potential of the HD-MEA platform is magnified, offering profound insights into the intricacies of brain functions in both healthy and pathological conditions.

In essence, the HD-MEA platform, when integrated with the detailed protocols and computational tools discussed, offers a transformative approach to understanding the intricate workings of the brain. By capturing large-scale, multiscale, and multimodal dynamics, it provides invaluable insights into processes such as learning, memory, and information processing. Moreover, its application in in-vitro human iPSC networks has the potential to revolutionize drug screening and personalized medicine. However, while this platform represents a significant advancement in neuroscience research, it is crucial to acknowledge and address the inherent technical challenges. With ongoing refinement and the integration of advanced computational tools, the HD-MEA platform stands poised to usher in a new era of precise diagnostic tools, the identification of specific biomarkers, and targeted therapies for neurological disorders.

## Disclosures

The authors declare no competing or financial interests.

## Acknowledgments

This study was supported by institutional funds (DZNE), the Helmholtz Association within the Helmholtz Validation Fund (HVF-0102), and the Dresden International Graduate School for Biomedicine and Bioengineering (DIGS-BB). We would also like to acknowledge the platform for behavioral animal testing at the DZNE-Dresden (Alexander Garthe, Anne Karasinsky, Sandra Günther, and Jens Bergmann) for their support. We would like to acknowledge that a portion of Figure 1 was created using the platform BioRender.com.

## References

1. Hebb, D. O. *The Organization of Behavior; A Neuropsychological Theory*. Wiley, New York (1949).
2. Cossart, R., Gareil, S. Step by step: cells with multiple functions in cortical circuit assembly. *Nat Rev Neurosci.* **23**, 395-410 (2022).
3. Carrillo-Reid, L., Yuste, R. Playing the piano with the cortex: role of neuronal ensembles and pattern completion in perception and behavior. *Curr Opin Neurobiol.* **64**, 89-95 (2020).
4. Buzsáki, G. Large-scale recording of neuronal ensembles. *Nat Neurosci.* **7**, 446-451 (2004).
5. Buzsáki, G. Neural Syntax: Cell assemblies, synapsembles, and readers. *Neuron.* **68** (3), 362-385 (2010).
6. Huang, Y., Williams, J. C., Johnson, S. M. Brain slice on a chip: opportunities and challenges of applying

- microfluidic technology to intact tissues. *Lab Chip*. **12** (12), 2103-2117 (2012).
7. Cho, S., Wood, A., Bowlby, M. Brain slices as models for neurodegenerative disease and screening platforms to identify novel therapeutics. *Curr Neuropharmacol*. **5** (1), 19-33 (2007).
  8. Bliss, T. V. P., Collingridge, G. L. A synaptic model of memory: long-term potentiation in the hippocampus. *Nature*. **361**, 31-39 (1993).
  9. Anderson, P., Morris, R., Amaral, D., Bliss, T., O'Keefe, L. *The Hippocampus Book*. Oxford University Press, New York (2006).
  10. Lisman, J. et al. Viewpoints: how the hippocampus contributes to memory, navigation and cognition. *Nat Neurosci*. **20**, 1434-1447 (2017).
  11. Mori, K., Nagao, H., Yoshihara, Y. The olfactory bulb: Coding and processing of odor molecule information. *Science*. **286** (5440), 711-715 (1999).
  12. Buck, L., Axel, R. A novel multigene family may encode odorant receptors: A molecular basis for odor recognition. *Cell*. **65** (1), 175-187 (1991).
  13. Bushdid, C., Magnasco, M. O., Vosshall, L. B., Keller, A. Humans can discriminate more than 1 trillion olfactory stimuli. *Science*. **343** (6177), 1370-1372 (2014).
  14. Kempermann, G. Why new neurons? Possible functions for adult hippocampal neurogenesis. *J Neurosci*. **23** (3), 635-638 (2003).
  15. Aimone, J. B., Wiles, J., Gage, F. H. Computational influence of adult neurogenesis on memory encoding. *Neuron*. **61** (2), 187-202 (2009).
  16. Nithianantharajah, J., Hannan, A. J. Enriched environments, experience-dependent plasticity and disorders of the nervous system. *Nat Rev Neurosci*. **7**, 697-709 (2006).
  17. Takahashi, K. et al. Induction of pluripotent stem cells from adult human fibroblasts by defined factors. *Cell*. **131** (5), 861-872 (2007).
  18. Espuny-Camacho, I. et al. Pyramidal neurons derived from human pluripotent stem cells integrate efficiently into mouse brain circuits in vivo. *Neuron*. **77** (3), 440-456 (2013).
  19. Rajamohan, D. et al. Current status of drug screening and disease modelling in human pluripotent stem cells. *Bioessays*. **35** (3), 281-298 (2013).
  20. Heilker, R., Traub, S., Reinhardt, P., Schöler, H. R., Sternecker, J. iPSC cell derived neuronal cells for drug discovery. *Trends Pharmacol Sci*. **35** (10), 510-519 (2014).
  21. Zhao, S. R., Mondéjar-Parreño, G., Li, D., Shen, M., Wu, J. C. Technical applications of microelectrode array and patch clamp recordings on human induced pluripotent stem cell-derived cardiomyocytes. *J Vis Exp*. **186**, e64265 (2022).
  22. Hamill, O. P., McBride, D. W. Induced membrane hypo/hyper-mechanosensitivity: A limitation of patch-clamp recording. *Annu Rev Physiol*. **59**, 621-631 (1997).
  23. Manz, K. M., Siemann, J. K., McMahon, D. G., Grueter, B. A. Patch-clamp and multi-electrode array electrophysiological analysis in acute mouse brain slices. *STAR Protoc*. **2** (2), 100442 (2021).
  24. Lee, C. H., Park, Y. K., Lee, K. Recent strategies for neural dynamics observation at a larger scale and wider scope. *Biosens Bioelectron*. **240**, 115638 (2023).

25. Urai, A. E., Doiron, B., Leifer, A. M., Churchland, A. K. Large-scale neural recordings call for new insights to link brain and behavior. *Nat Neurosci.* **25** (1), 11-19 (2022).
26. Hu, X., Khazada, S., Klütsch, D., Calegari, F., Amin, H. Implementation of biohybrid olfactory bulb on a high-density CMOS-chip to reveal large-scale spatiotemporal circuit information. *Biosens Bioelectron.* **198**, 113834 (2022).
27. Amin, H., Marinaro, F., Tonelli, D. D. P., Berdondini, L. Developmental excitatory-to-inhibitory GABA-polarity switch is disrupted in 22q11.2 deletion syndrome: A potential target for clinical therapeutics. *Sci Rep.* **7** (1), 15752 (2017).
28. Amin, H., Nieuw, T., Lonardoni, D., Maccione, A., Berdondini, L. High-resolution bioelectrical imaging of A $\beta$ -induced network dysfunction on CMOS-MEAs for neurotoxicity and rescue studies. *Sci Rep.* **7** (1), 2460 (2017).
29. Emery, B. A., Hu, X., Khazada, S., Kempermann, G., Amin, H. High-resolution CMOS-based biosensor for assessing hippocampal circuit dynamics in experience-dependent plasticity. *Biosens Bioelectron.* **237**, 115471 (2023).
30. Amin, H. et al. Electrical responses and spontaneous activity of human iPS-derived neuronal networks characterized for 3-month culture with 4096-electrode arrays. *Front Neurosci.* **10**, 121 (2016).
31. Lonardoni, D. et al. Recurrently connected and localized neuronal communities initiate coordinated spontaneous activity in neuronal networks. *PLoS Comput Biol.* **13** (7), e1005672 (2017).
32. Emery, B. A. et al. Large-scale multimodal recordings on a high-density neurochip: Olfactory bulb and hippocampal networks. *2022 44th Annual International Conference of the IEEE Engineering in Medicine & Biology Society (EMBC), Glasgow, Scotland, United Kingdom.* 3111-3114 (2022).
33. Rossi, L., Emery, B. A., Khazada, S., Hu, X., Amin, H. Pharmacologically and electrically-induced network-wide activation of olfactory bulb with large-scale biosensor. *2023 IEEE BioSensors Conference (BioSensors), London, United Kingdom.* 1-4 (2023).
34. Emery, B. A. et al. Recording network-based synaptic transmission and LTP in the hippocampal network on a large-scale biosensor. *2023 IEEE BioSensors Conference (BioSensors), London, United Kingdom.* 1-4 (2023).
35. Hierlemann, A., Frey, U., Hafizovic, S., Heer, F. Growing cells atop microelectronic chips: Interfacing electrogenic cells in vitro with CMOS-based microelectrode arrays. *Proceedings of the IEEE.* **99** (2), 252-284 (2011).
36. Berdondini, L. et al. Active pixel sensor array for high spatio-temporal resolution electrophysiological recordings from single cell to large scale neuronal networks. *Lab Chip.* **9**, 2644-2651 (2009).
37. Siegle, J. H., Hale, G. J., Newman, J. P., Voigts, J. Neural ensemble communities: open-source approaches to hardware for large-scale electrophysiology. *Curr Opin Neurobiol.* **32**, 53-59 (2015).
38. Amin, H., Maccione, A., Zordan, S., Nieuw, T., Berdondini, L. High-density MEAs reveal lognormal firing patterns in neuronal networks for short and long term recordings. in *2015 7th International IEEE/EMBS*

- Conference on Neural Engineering (NER), Montpellier, France. 1000-1003 (2015).*
39. Altuntac, E. et al. Bottom-up neurogenic-inspired computational model. in *2023 IEEE BioSensors Conference (BioSensors), London, United Kingdom. 1-4 (2023).*
  40. Maccione, A. et al. A novel algorithm for precise identification of spikes in extracellularly recorded neuronal signals. *J Neurosci Methods. 177 (1), 241-249 (2009).*
  41. Welch, P. D. The use of fast Fourier transform for the estimation of power spectra: A method based on time averaging over short, modified periodograms. *IEEE Transactions on Audio and Electroacoustics. 15 (2), 70-73 (1967).*
  42. Eggermont, J. J., Munguia, R., Pienkowski, M., Shaw, G. Comparison of LFP-based and spike-based spectrotemporal receptive fields and cross-correlation in cat primary auditory cortex. *PLoS One. 6 (5), e20046 (2011).*
  43. Damos, P. Using multivariate cross correlations, Granger causality and graphical models to quantify spatiotemporal synchronization and causality between pest populations. *BMC Ecol. 16, 33 (2016).*
  44. Kaminski, M. J., Blinowska, K. J. A new method of the description of the information flow in the brain structures. *Biol Cybern. 65, 203-210 (1991).*
  45. Pastore, V. P., Massobrio, P., Godjowski, A., Martinoia, S. Identification of excitatory-inhibitory links and network topology in large-scale neuronal assemblies from multi-electrode recordings. *PLoS Comput Biol. 14 (8), e1006381 (2018).*
  46. Amin, H., Dipalo, M., De Angelis, F., Berdondini, L. Biofunctionalized 3D nanopillar arrays fostering cell guidance and promoting synapse stability and neuronal activity in networks. *ACS Appl Mater Interfaces. 10 (17), 15207-15215 (2018).*
  47. Woepfel, K., Yang, Q., Cui, X. T. Recent advances in neural electrode-tissue interfaces. *Curr Opin Biomed Eng. 4, 21-31 (2017).*
  48. Steinmetz, N. A., Koch, C., Harris, K. D., Carandini, M. Challenges and opportunities for large-scale electrophysiology with Neuropixels probes. *Curr Opin Neurobiol. 50, 92-100 (2018).*
  49. Siegle, J. H., Hale, G. J., Newman, J. P., Voigts, J. Neural ensemble communities: open-source approaches to hardware for large-scale electrophysiology. *Curr Opin Neurobiol. 32, 53-59 (2015).*
  50. Freeman, J. Open source tools for large-scale neuroscience. *Curr Opin Neurobiol. 32, 156-163 (2015).*
  51. Stevenson, I. H., Kording, K. P. How advances in neural recording affect data analysis. *Nat Neurosci. 14 (2), 139-142 (2011).*